CHAPTER 6

BUOYANT CONVECTION FROM ISOLATED SOURCES

The buoyancy effects discussed so far have for the most part been stabilizing, or have been assumed to produce a small modification of an existing turbulent flow. Now we turn to convective flows, in which buoyancy forces play the major role because they are the source of energy for the mean motion itself. The usual order of presentation will be reversed: it is convenient to set aside for the present the discussion of the mean properties of a convecting region of large horizontal extent, and flows near solid bodies, and in this chapter to treat various models of the individual convective elements which carry the buoyancy flux. (See Turner (1969*a*) for a review of this work and a more extensive bibliography.)

Such models can be broadly divided into two groups, those which assume the motion to be in the form of 'plumes' or of 'thermals'. (See fig. 6.1.) In both of them motions are produced under gravity by a density contrast between the source fluid and its environment; the velocity and density variations are interdependent, and occupy a limited region above or below the source. *Plumes*, sometimes called buoyant jets, arise when buoyancy is supplied steadily and the buoyant region is continuous between the source and the level of interest. The term *thermal* is used in the sense which has become common in the meteorological literature to denote suddenly released buoyant elements. The buoyancy remains confined to a limited volume of fluid, which, as it rises, loses its connection with the source which produced it. Other models have some features in common with both of these. (See §6.3.3 and fig. 6.1.)

Both plumes and thermals can be axisymmetric or two-dimensional, and each case will be discussed here with varying degrees of detail. The Boussinesq approximation will be used throughout, neglecting (potential) density differences except where they occur in

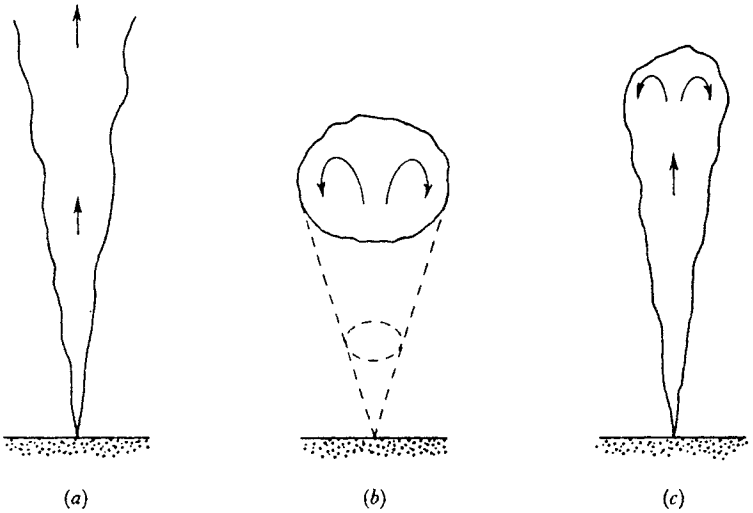

Fig. 6.1. Sketches of the various convection phenomena described in this chapter: (*a*) plume, (*b*) thermal, (*c*) starting plume. The arrows indicate the direction of mean motion. (From Turner 1969*a*.)

the buoyancy terms. We will discuss the motion with buoyancy taken as positive upwards, i.e. as if heated air were rising through the atmosphere, though of course the direction of motion is immaterial to the dynamics, and laboratory experiments often for convenience use plumes of salt water descending through a tank of fresh water.

Most of the results described here are similarity solutions of the kind described by Batchelor (1954*a*). Dimensional arguments are very powerful tools for investigating the overall properties of such flows, and when combined with numerical values of parameters obtained from laboratory experiments, they allow one to make predictions about the flow pattern and density distribution over a very wide range of scales. Detailed theories of these motions are much less well developed, however, and there are important natural flows (e.g. large convective clouds – see §6.4.1) which are not adequately described by similarity theory but for which there is at present no alternative model.

6.1. Plumes in a uniform environment

The major parameter governing the flow above a small axisymmetric source of buoyancy can be defined as

$$F_0 = 2\pi \int_0^\infty wg'r\,\mathrm{d}r, \tag{6.1.1}$$

where w is the vertical velocity, $g' = g\rho'/\rho_0$ and r is the radial distance from a vertical line above the source. Thus $\rho_0 F_0$ is the total weight deficiency produced per unit time at the source, and F_0 must remain constant with height z in an environment of constant density ρ_0 (though w will decrease and the radial lengthscale b increase with increasing distance z above the source). Such flows can stay laminar only for very low values of F_0 – even the plume from a cigarette becomes unstable after rising a short distance – and attention will be concentrated here on the practically more important turbulent plumes.

6.1.1. *Axisymmetric turbulent plumes*

Basic to the understanding of all free turbulent flows is the process of 'entrainment' or mixing of outside fluid into the plume. It is observed that (like jets) turbulent plumes have a sharp boundary separating nearly uniform turbulent buoyant fluid from the surroundings, as pictured in the photograph of fig. 6.2*a* pl. XIV. This boundary is indented by large eddies and the mixing process takes place in two stages, the engulfing of external fluid by the large eddies, followed by rapid smaller scale mixing across the central core. The vertical velocity and the turbulence measured at a fixed point off the axis have an intermittent character, since the plume is waving about and a measuring instrument spends part of its time in the fully turbulent fluid, and part outside it. Though an instantaneous profile across a plume is sharp-edged, the time averaged profiles of velocity and temperature are smoother, and can be well fitted by Gaussian curves.

A detailed theory of the mechanism of entrainment (and a comparison between different free flows) has been given by Townsend (1970), but the above simplified picture is sufficient for the

present purpose. The *similarity* of the profiles at all heights above the source is the main assumption made here; no information is obtained from similarity theory about their form, and the particular choice made is a matter of convenience only. In the following we will often use the simplest 'top hat' shape (i.e. the properties have one constant value inside the plume, and another outside it). This is equivalent to replacing the mass and momentum fluxes by mean values defined as integrals across the plume, and does not imply any physical assumption. The rate of spread is governed by the large scale structure of the turbulence generated by the motion of the plume itself, and the assumption of similarity means that this must have the same relation to the mean flow whatever the scale of motion. Provided the Reynolds number $Re = wb/\nu$ is large enough, neither the molecular properties ν and κ of the fluid nor Re itself can enter directly into the determination of the overall properties of a turbulent plume.

The parameters defining the behaviour of an axisymmetric turbulent plume can therefore be taken as F_0, z and r. A dimensional analysis shows immediately that

$$\left.\begin{aligned} w &= F_0^{\frac{1}{3}} z^{-\frac{1}{3}} f_1\left(\frac{r}{b}\right), \\ g' &= F_0^{\frac{2}{3}} z^{-\frac{5}{3}} f_2\left(\frac{r}{b}\right), \\ b &= \beta z, \end{aligned}\right\} \tag{6.1.2}$$

where β is a constant to be defined for particular profiles. The turbulent plume thus has a conical form, with apex at the source. Such a point source is of course physically unrealistic, since (6.1.2) implies that both w and g' become infinite as $z \to 0$. At some distance above a real source, however, the flow behaves as if it came from a 'virtual point source' below, and the point source remains a useful theoretical concept, provided (6.1.2) are applied to plumes which rise to a height of many diameters above the source.

The actual form of f_1 and f_2 must be obtained using either more detailed theories (all of which entail some questionable assumptions about the turbulence distributions across the plume), or directly by experiment. For example, the experiments of Rouse, Yih and Humphreys (1952), made using a heat source in a large room, both

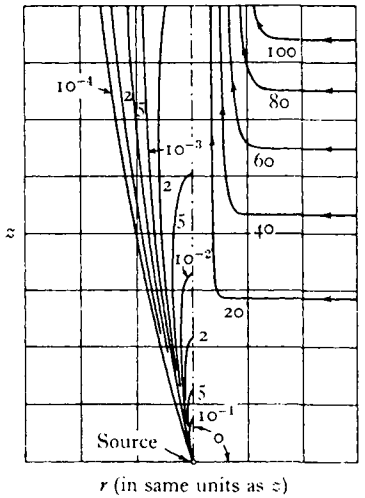

Fig. 6.3. Mean isotherms (left) and streamlines (right) for turbulent convection from a maintained point source. The numbers on the isotherms are relative values of $\Delta\rho/\rho_0$, and those on the streamlines are relative values of the Stokes stream function (from Rouse, Yih and Humphreys 1952).

confirmed the above forms of dependence on z and indicated that the mean profiles were closely Gaussian. The results can be represented to the experimental accuracy by

$$\left.\begin{aligned} w &= 4.7F_0^{\frac{1}{3}}z^{-\frac{1}{3}}\exp(-96r^2/z^2),\\ g' &= 11F_0^{\frac{2}{3}}z^{-\frac{5}{3}}\exp(-71r^2/z^2). \end{aligned}\right\} \qquad (6.1.3)$$

The corresponding mean isotherms and streamlines in the plume are reproduced in fig. 6.3; these show that the width of the region containing turbulent buoyant fluid is always expanding, but the *visible* region (containing concentrations above a certain minimum in a plume marked by smoke, for example) will at first expand and then contract and disappear. The value of β found experimentally (and used in the plot) will be discussed in the next section. Note that (6.1.3) implies a slightly greater (mean) spread of buoyancy relative to momentum.

The above solutions show that there is a flow from the environment into the turbulent plume, since the mass flux is clearly increasing with height. This radial flow at large r is not taken into

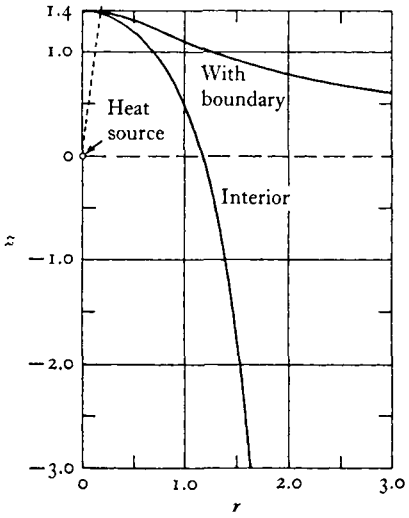

Fig. 6.4. Streamlines for inflow into a plume rising from a point heat source located on the horizontal boundary or in the interior of a large region of uniform fluid. (From Taylor 1958.)

account in (6.1.3) which refer only to the narrow region of strong vertical motion, but it may be found using a method introduced by Taylor (1958). As far as the external fluid is concerned, a plume (or jet) can be replaced by a line of sinks along the axis, and the inflow calculated approximately by potential flow theory. The sink distribution must be chosen to match the calculated inflow at each level, and varies with the kind of flow; for axisymmetric buoyant plumes, the increase in mass flux with z implied by (6.1.2) gives a sink strength proportional to $z^{\frac{5}{3}}$. The forms of typical streamlines computed for the two cases where the point source is on a plane, or in the middle of an unbounded region of uniform fluid, are reproduced in fig. 6.4; they show that the fluid entering the plume may have come from very different parts of the environment, according to the shape of the region in which convection is taking place.

6.1.2. *The entrainment assumption*

As Batchelor (1954*a*) pointed out, this increasing vertical flow in a plume also implies that there is a mean inflow velocity across the

boundary which varies as $z^{-\frac{1}{3}}$. That is, the linear spread of radius with height implies that the mean inflow velocity across the edge of the plume is proportional to the local mean upward velocity (6.1.2). This statement, regarded now as the basic assumption, was first introduced by Sir Geoffrey Taylor, and was used by Morton, Taylor and Turner (1956) to discuss cases where similarity solutions of the above form do not exist. It is in fact another type of similarity assumption, which implies that there is the same kind of turbulent structure and balance of forces at each height. It is simple and powerful, and is to some extent justified by its success in a variety of contexts, but its range of validity must always be examined carefully. It has been argued by Morton (1968), for example, that for flows where the equilibrium structure has not been attained, the entrainment should be related not to the mean velocity but to the Reynolds stress, and Telford (1966, 1970) has proposed that the local level of turbulence should be used as the velocity scale. The detailed analysis of the entrainment process by Townsend (1970) shows that none of these is precisely satisfied, but nevertheless they remain useful approximations.

When the simplest entrainment assumption is made, so that the inflow velocity is taken to be some fraction α of the upward velocity, the equations of conservation of mass, momentum and buoyancy can be reduced to the form

$$\left.\begin{aligned} \frac{\mathrm{d}(b^2\overline{w})}{\mathrm{d}z} &= 2\alpha b\overline{w}, \\ \frac{\mathrm{d}(b^2\overline{w}^2)}{\mathrm{d}z} &= b^2 g', \\ \frac{\mathrm{d}(b^2\overline{w}g')}{\mathrm{d}z} &= -b^2\overline{w}N^2(z). \end{aligned}\right\} \tag{6.1.4}$$

The neglect of a pressure term in the second of these equations can be rigorously justified provided the plume remains narrow. With a later use in mind, an arbitrary density variation in the environment has been allowed for; $g' = g(\rho_0 - \rho)/\rho_1$ is calculated using the local density difference between the plume ρ and its environment ρ_0 at the height z and some standard density ρ_1 in the environment, and $N^2 = (-g/\rho_1)(\mathrm{d}\rho_0/\mathrm{d}z)$ is the square of the local buoyancy

frequency. The velocity $\overline{w}$ and width b are defined by integrating the mass and momentum fluxes across the plume:

$$\overline{w}b^2 = 2\int_0^\infty w(r)r\,\mathrm{d}r, \quad \overline{w}^2b^2 = 2\int_0^\infty w^2(r)r\,\mathrm{d}r, \tag{6.1.5}$$

i.e. an equivalent 'top hat' profile is implied in (6.1.4).

When the environment is of uniform density, $N = 0$, so the third equation in (6.1.4) is a formal statement of the fact that the buoyancy flux is constant, $b^2\overline{w}g' = F_0/\pi = F$ say. The solution of the other two equations, with the boundary conditions that the mass and momentum fluxes are zero at the source, is entirely equivalent to the similarity solution (6.1.2). The multiplying constants such as β are now, however, all given explicitly in terms of the 'entrainment constant' α:

$$\left.\begin{aligned} b &= \tfrac{6}{5}\alpha z, \\ \overline{w} &= \frac{5}{6\alpha}(\tfrac{9}{10}\alpha F)^{\frac{1}{3}}z^{-\frac{1}{3}}, \\ g' &= \frac{5F}{6\alpha}(\tfrac{9}{10}\alpha F)^{-\frac{1}{3}}z^{-\frac{5}{3}}. \end{aligned}\right\} \tag{6.1.6}$$

Allowance can be made for different widths of the velocity and buoyancy profiles with little increase in complication.

It will be seen later (§6.4) how other more general kinds of plumes, having different rates of variation of buoyancy with height, can be treated by the same method. For the present it will suffice to comment on two of the consequences of the equations (6.1.4), which hold regardless of the form of $N^2(z)$ and g'. The mass continuity equation implies that the *proportional* rate of entrainment or change of mass flux (or, in the Boussinesq approximation, the volume flux V) is inversely proportional to the radius, i.e.

$$V^{-1}(\mathrm{d}V/\mathrm{d}z) = 2\alpha/b. \tag{6.1.7}$$

The first two equations may be combined to express the rate of spread as

$$\mathrm{d}b/\mathrm{d}z = 2\alpha - (bg'/2\overline{w}^2). \tag{6.1.8}$$

Thus the half angle of spread ($\frac{6}{5}\alpha$) of a plume in a uniform environment is proportional to the entrainment constant, but is less than

the angle 2α for a non-buoyant jet (with $g' = 0$), for the same value of α. (See fig. 6.5, which is discussed further in the following section.)

The numerical value to be chosen for α cannot be obtained theoretically (though comparisons between different kinds of flow have been made), and it must be taken from laboratory experiments. Morton (1959*b*) adopted a value of 0.116 for top hat profiles, based on measurements in non-buoyant jets (for Gaussian profiles, if the scale of w is defined to be the velocity on the axis, and b the radial distance to the point where the velocity is reduced by a factor e^{-1}, then it follows from the definitions (6.1.5) that the corresponding entrainment constant $\alpha_G = 2^{-\frac{1}{2}}\alpha$).

Ricou and Spalding (1961) have found a value of α for jets closer to 0.08; they used a direct method of measuring the inflow which avoids the errors introduced by integrating across measured profiles. Their experiments also suggested that the entrainment constant for buoyant plumes is somewhat greater than for jets. A value of $\alpha = 0.12$ for plumes is deduced from the profiles (6.1.3), but direct results of comparable accuracy to those in jets are not yet available for plumes. Since α does not enter sensitively into many calculations, a fixed value of say $\alpha = 0.10$ (or $\alpha_G = 0.07$) might be adopted in all cases until more definitive measurements become available.

6.1.3. *Forced plumes*

Although it is often useful to interpret observations on plumes from finite sources in terms of one arising from an equivalent virtual point source of buoyancy alone, it is not necessary always to do so. The equations (6.1.4) can be solved with any initial values of radius and velocity (always bearing in mind the reservations about the validity of the entrainment assumption in the 'developing' part of the flow). Another important case is the turbulent flow generated by a finite source which emits fluxes of mass and momentum at a steady rate, as well as buoyancy. Morton (1959*a*) has shown that this general flow, which he has called the forced plume (and includes non-buoyant jets and pure plumes as special cases) can be related to the flow from a virtual point source of buoyancy and momentum only.

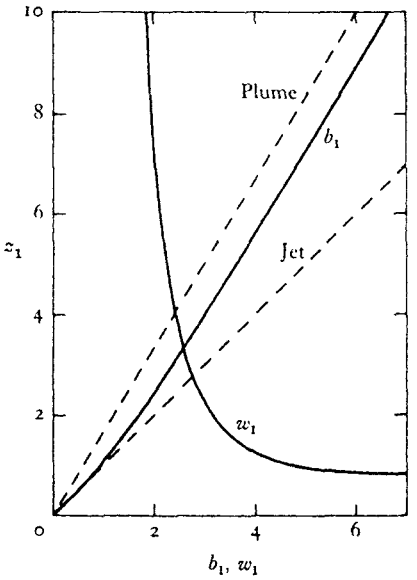

Fig. 6.5. The behaviour of a forced plume in a uniform environment, showing the non-dimensional radius b_1 and vertical velocity w_1 as functions of height. The initial spread is like a jet, but later approaches that characteristic of plumes. (From Morton 1959*a*.)

Two physical parameters are now specified at the source, the rates of discharge of buoyancy $\rho_1 F_0$ and momentum $\rho_1 M_0$ say. All the variables of the problem can be scaled in terms of these, and one can write

$$\left.\begin{aligned} z &= \alpha^{-\frac{1}{2}} |M_0|^{\frac{3}{4}} |F_0|^{-\frac{1}{2}} z_1, \\ b &= \alpha^{\frac{1}{2}} |M_0|^{\frac{3}{4}} |F_0|^{-\frac{1}{2}} b_1, \\ \overline{w} &= \alpha^{-\frac{1}{2}} |M_0|^{-\frac{1}{4}} |F_0|^{\frac{1}{2}} w_1, \end{aligned}\right\} \tag{6.1.9}$$

where z_1, b_1 and w_1 are non-dimensional variables. The equations (6.1.4) reduce to a non-dimensional pair in the variables $(b_1 w_1)$ and $(b_1^2 w_1)$, with boundary conditions $b_1 w_1 = \pm 1$ and $b_1^2 w_1 = 0$ at $z = 0$.

This formulation includes the possibility that F_0 and M_0 can have either sign; two cases will be discussed as examples. When both the buoyancy and momentum fluxes are directed upwards, the non-dimensional solutions for radius and velocity are shown in fig. 6.5. The rate of spread is at first like that in a pure jet, but as the momentum generated by buoyancy dominates over the initial momentum,

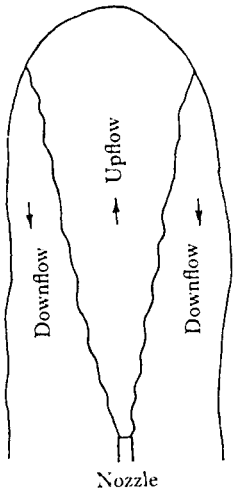

Fig. 6.6. Sketch of the up and downflow regions in a heavy salt jet projected upwards. The outer boundary is approximately to scale, but the inner boundary is schematic only. (From Turner 1966.)

the spread (for given α, of course) becomes smaller and approaches that of a plume. This behaviour must be kept in mind in any experiments designed to *measure* α in plumes, since any extra momentum at the source could have an effect that might be interpreted as a larger α. It will also be of importance in a stable environment (§6.4.3).

When the source fluid is *heavier* than the environment, but its initial momentum is upwards, then the momentum is continually being decreased by the buoyancy forces, until it becomes zero and then begins to increase downwards. The solution of the equations derived from (6.1.4) can be used to estimate the maximum height to which fluid first rises, but after that the model becomes unrealistic. Experiments (Turner 1966) show that in this case the heavy fluid falls back in an annular region surrounding the upflow (see fig. 6.6), and the simple theory does not allow for the mixing between the two streams moving in opposite directions. It is observed, however, that in the steady state the plume top fluctuates slightly about a height z_m which is a constant fraction (0.70) of that to which it first rises, and experiments using salt water injected into fresh have

confirmed the relation $z_m = 1.85\, M_0^{\frac{3}{4}} F_0^{-\frac{1}{2}}$, which is the form to be expected from (6.1.9).

There is a useful alternative interpretation of these results, which is related to the analysis given in §6.2.2. In an actual experiment fluid is ejected from a nozzle of radius r_0 with velocity U_0, so $M_0 = \pi r_0^2 U_0^2$ and $F_0 = \pi g_0' r_0^2 U_0$. For the experiment with heavy fluid, the maximum height z_m may be written as

$$\frac{z_m}{r_0} \propto \frac{U_0}{(g_0' r_0)^{\frac{1}{2}}} = F = Ri_0^{-\frac{1}{2}}. \tag{6.1.10}$$

That is, the ratio of the height of rise to the radius of the nozzle is directly proportional to an internal Froude number F based on the initial properties of the negatively buoyant jet.† The Froude number is also relevant, of course, in the case where both buoyancy and initial momentum are directed upwards. A pure plume in neutral surroundings has a particular *constant* value of the Froude number (with the definitions and scaling used in (6.1.6), this is $(\frac{8}{5}\alpha)^{-\frac{1}{2}}$, but the actual value is less important than the fact that it exists). If fluid is ejected from a finite source with this value of F, it will behave exactly like a plume originating from a point source below; if it comes out with different properties, these will change so as to approach the value of F appropriate to a plume. A jet-like flow initially has $F \to \infty$ and gives the most rapid mixing of an effluent with its environment, whereas a plume accelerating fluid from rest ($F = 0$ at the source) results in a more rapid removal of plume fluid from the neighbourhood of the source.

6.1.4. *Vertical two-dimensional plumes*

Analogous results can be obtained for line sources of buoyancy in uniform surroundings, using similarity arguments (based now on the buoyancy flux per unit length, $\rho_0 A$ say) or the equivalent entrainment assumption. The rate of spread of the transverse dimension x is again linear with height, and the profiles nearly Gaussian; dimensional arguments show that the velocity scale is independent of height z and the density difference varies inversely as z. The full

† The use of the same symbol F for Froude number and buoyancy flux is unfortunate here; in no other section do they occur together.

solutions, with the profile shapes suggested by the experiments of Rouse, Yih and Humphreys (1952) are

$$\left.\begin{aligned} w &= 1.8A^{\frac{1}{3}}\exp(-32x^2/z^2), \\ g' &= 2.6A^{\frac{2}{3}}z^{-1}\exp(-41x^2/z^2). \end{aligned}\right\} \tag{6.1.11}$$

The accuracy of such experiments is not high enough to be sure that the suggested greater spread of velocity relative to buoyancy is real, and indeed the waving about of these plumes makes the estimate of an entrainment constant from the profiles very inaccurate. A direct estimate of entrainment is available here too (from the experiments of Ellison and Turner (1959) which will be described more fully in the following section); these give the value of $\alpha = 0.08$ for top hat profiles.

Line plumes arise in several applications of practical importance. Priestley (1959) has suggested that the sources of warm air near the ground get drawn out into lines down wind, so that typical convection elements are like two-dimensional symmetric plumes. Artificial plumes formed by lines of burners have been used in attempts to disperse fog from aircraft runways. Examples in the ocean are the discharge of sewage from a manifold laid on the bottom, and the 'bubble breakwater' invented by Sir Geoffrey Taylor. This last example arose from the suggestion that if a curtain of air bubbles is forced from a horizontal pipe some distance below the surface of the sea, then waves will be damped by the surface outflow of water driven upwards by the bubbles. The point of interest here is that the flux of density deficiency due to the small bubbles can be treated in exactly the same way as that due to fresh water rising through salt water, or to heat in a turbulent plume in air, since in each case the molecular diffusivity is irrelevant. The relevant flux can be calculated from the total volume of air released; if the bubbles are rising at terminal velocity, the whole of their buoyancy is transmitted to the water around them, and provided they are small they are transported about by the turbulence in the plume. In the same way sediment, if its concentration is not too great, can drive 'turbidity currents' by changing the buoyancy of the water containing it. This last example will be treated at greater length in the following section.

6.2. Inclined plumes and turbulent gravity currents

We now come to a phenomenon which can be regarded as a generalization of the one just treated – a two-dimensional turbulent plume, but now on a slope at an arbitrary angle θ to the horizontal (see fig. 6.7). Related topics have already received some attention, the frictionless flow of a heavy fluid under a lighter one, and its relation to hydraulic theory in chapter 3, and the laminar viscous flow and its stability in chapter 4. The new problems introduced when the flow is turbulent and can mix with the environment, assumed to be non-turbulent, are of sufficient importance to require extra discussion here. There is also a close connection with the turbulent stratified flows mentioned in § 5.1, whose discussion we have deferred till this section so that both the driving and the stabilizing aspects of the density gradients could logically be considered together.

There are many situations in nature where such flows can arise. Katabatic winds in the atmosphere occur when air cooled by contact with cold ground flows downhill. Similar currents arise in the ocean, for example when cold water from Arctic regions flows along the bottom under warmer water. Heavy layers can also be formed because of the extra weight of suspended solids; turbidity currents in the ocean (Johnson 1963) and 'density currents' in reservoirs arise from this cause. In the atmosphere too, some dust storms and powder snow avalanches are driven by the weight of the suspended material (see fig. 3.14 pl. VI) though in these cases the advance of the 'front', or leading edge of the disturbance, is of more importance than the steady flow behind. Gravity currents can equally well be formed by a lighter layer under a sloping roof, as in the example of a layer of methane flowing along the roof of a mine, which was mentioned in § 5.3.3.

6.2.1. *A modified entrainment assumption*

When a two-dimensional plume, or gravity current, is inclined to the vertical there will be a component of gravity acting normal to the entraining edge, so that gravity will inhibit mixing into the plume as well as driving it along the slope. A measure of the stabilizing effect of the density gradient relative to the shear is again an overall

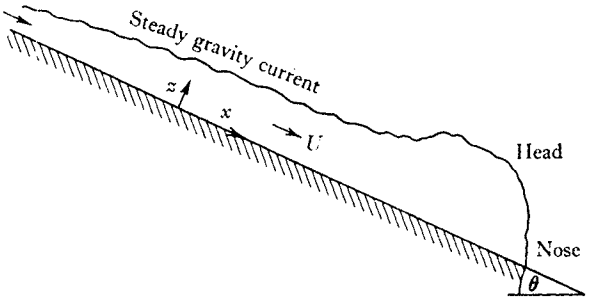

Fig. 6.7. Sketch of a gravity current on a slope, with an initial head followed by a steady layer flow.

Richardson number, which can be defined for the present purposes as

$$Ri_0 = \frac{g'h\cos\theta}{U^2} = \frac{A\cos\theta}{U^3}, \tag{6.2.1}$$

where U is the mean velocity down the slope and h the depth, defined by integrals analogous to (6.1.5)

$$Uh = \int_0^\infty u\,\mathrm{d}z, \quad U^2h = \int_0^\infty u^2\,\mathrm{d}z, \tag{6.2.2}$$

and $A = g'hU$ is the buoyancy flux per unit width (cf. §5.3.2).

The new assumption required when the plume is inclined (Ellison and Turner 1959) is that the entrainment parameter is not now the constant α appropriate to vertical plumes, but that it can be a function $E(Ri_0)$ of the Richardson number (6.2.1). If the assumption of similarity of profiles is retained, relations of the form (6.1.11) will apply, but with the magnitudes modified because of the slope. Gravity currents will still spread linearly with distance x, their mean velocity will be constant and proportional to $A^{\frac{1}{3}}$, and the density difference will be inversely proportional to x.

The mass continuity equation (with the ambient fluid at rest) is

$$\frac{\mathrm{d}(Uh)}{\mathrm{d}x} = EU, \tag{6.2.3}$$

where E is now a function of Ri_0. In the simplest case, when one can follow the method used for vertical plumes and regard bottom friction as unimportant compared with the stress at the edge due to entrainment, the momentum equation is just

$$\frac{\mathrm{d}(U^2h)}{\mathrm{d}x} = g'h\sin\theta. \tag{6.2.4}$$

(For the moment a 'profile constant', which could arise because of the form of the density distribution, is ignored.) It follows from the last two equations that for a flow dominated by the turbulent entrainment

$$E = Ri_0 \tan\theta. \tag{6.2.5}$$

Thus E is a strong function of slope, and is zero (except for the effects of bottom friction) at a finite value of Ri_0 when the bed becomes horizontal.

6.2.2. *Slowly varying flows*

In the general case, the momentum equation can be written

$$\frac{\mathrm{d}(U^2h)}{\mathrm{d}x} = -C_{\mathrm{D}}U^2 - \frac{1}{2}\frac{\mathrm{d}(S_1 g' h^2 \cos\theta)}{\mathrm{d}x} + S_2 g' h \sin\theta, \tag{6.2.6}$$

where C_{D} is the drag coefficient (cf. (3.2.7)), and S_1 and S_2 are profile constants defined by integrating across the plume. The terms on the right represent respectively the turbulent frictional drag on the bottom, the pressure force on the layer due to its changing depth (a term which was ignored in (6.2.4) and which is relatively less important), and the force of gravity accelerating the layer. If any variation of S_1, S_2 and θ with x is neglected (6.2.6) can be combined with (6.2.3) to give separate equations for $\mathrm{d}h/\mathrm{d}x$ and $\mathrm{d}Ri_0/\mathrm{d}x$. These are:

$$\frac{\mathrm{d}h}{\mathrm{d}x} = \frac{(2 - \frac{1}{2}S_1 Ri_0)E - S_2 Ri_0 \tan\theta + C_{\mathrm{D}}}{1 - S_1 Ri_0}, \tag{6.2.7}$$

$$\frac{h}{3Ri_0}\frac{\mathrm{d}Ri_0}{\mathrm{d}x} = \frac{(1 + \frac{1}{2}S_1 Ri_0)E - S_2 Ri_0 \tan\theta + C_{\mathrm{D}}}{1 - S_1 Ri_0}. \tag{6.2.8}$$

Equation (6.2.7) adds the effects of mixing to those earlier considered in deriving (3.2.8) using the 'hydraulic' assumptions. In the previous case, however, h and Ri_0 (or F) were directly connected through the equation of continuity; there was a certain depth at which $Ri_0 = 1$ and another depth for which $\mathrm{d}h/\mathrm{d}x = 0$, $\mathrm{d}Ri_0/\mathrm{d}x = 0$. In the present case where mixing can take place, the behaviour of Ri_0 is little different from that in ordinary hydraulics, but h is no longer connected uniquely with it. There is a particular value of

Ri_0 called the *normal* value Ri_n, determined by the slope and also by friction, for which the right-hand side of (6.2.8) vanishes and Ri_0 is constant along the slope; to determine Ri_n one must therefore know S_1 and S_2 and use measured values for E as a function of Ri_0.

The analogy with hydraulic theory may be pursued further. The forms of solution of (6.2.7) and (6.2.8) depend on the relative magnitudes of $S_1 Ri_0$ at the origin, $S_1 Ri_n$ and 1. The distinction can still be made between tranquil (subcritical) flow in which $S_1 Ri_0 > 1$ and the velocity of long internal waves on the layer is greater than the flow velocity, and shooting (supercritical) flow in which $S_1 Ri_0 < 1$ and disturbances are unable to propagate upstream. Experimentally, it appears that entrainment becomes small at $Ri_0 \approx 1$, so that all flows on small slopes may be treated approximately as if they did not mix (as was done in chapter 3). At the other extreme, on steep slopes both $S_1 Ri_0$ and $S_1 Ri_n$ are less than unity, and the flow is supercritical throughout. The adjustment to the 'normal' state is quite rapid; if the flow starts too slowly, gravity accelerates it, and if it starts too fast, increased mixing occurs until Ri approaches Ri_n. At this time the spread is linear with

$$\frac{dh}{dx} = E(Ri_n). \tag{6.2.9}$$

6.2.3. *Laboratory experiments and their applications*

The form of the entrainment function $E(Ri_0)$ must, as in the case of the entrainment constant for vertical plumes, be found by experiment. Two kinds of laboratory experiment have been used. The first consists of a horizontal turbulent surface jet above a heavier fluid, or a bottom current on a horizontal floor under a lighter layer, which is started with high velocity and low Ri_0 (and therefore in a 'supercritical' state). As it mixes and spreads out, its Richardson number increases towards a value where the flow is subcritical, and by assuming local equilibrium, E can be evaluated from the rate of spread at a number of intermediate values of Ri_0; the most important feature is a rapid fall of E with increasing Ri_0. (See fig. 6.8.) The relation between the velocity and depth during this process is

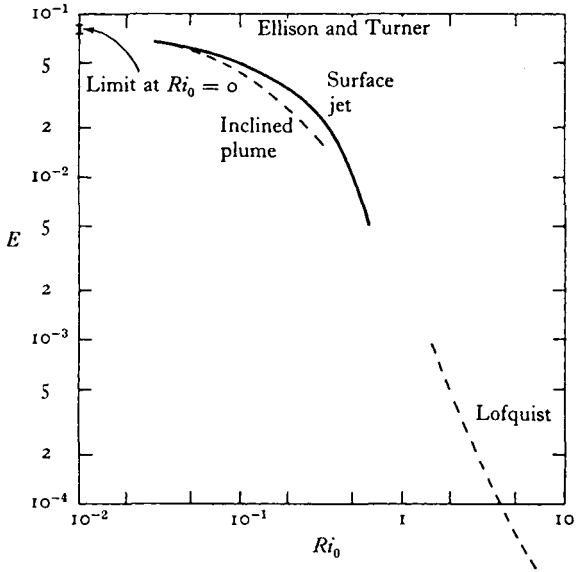

Fig. 6.8. Rate of entrainment into a turbulent stratified flow as a function of overall Richardson number, for two types of experiment described by Ellison and Turner (1959), and the experiments of Lofquist (1960).

obtained by integrating the momentum equation (6.2.6) with $\theta = 0$, $C_D = 0$ to give (when $S_1 = 1$)

$$\frac{h(1 + \frac{1}{2}Ri_0)}{Ri_0^{\frac{3}{2}}} = \text{const.} \qquad (6.2.10)$$

Wilkinson and Wood (1971) have shown that it is useful to interpret this region of flow adjustment as a kind of hydraulic jump, in which some of the kinetic energy lost from the mean flow is responsible for mixing. There is the important difference that the flow conditions on each side of the mixing region are not now uniquely related; a range of possible states can be attained downstream (for given values of h and Ri_0 upstream), depending on the nature of the downstream control. The maximum total entrainment occurs when $Ri_0 = 1$ downstream (or rather less when S_1 and S_2 are included), by which stage E has become negligible. If the flow downstream is controlled by a weir whose height is gradually increased, Ri_0 increases, a region of reversed flow moves upstream and the total mixing is reduced, until the jump is completely submerged and there is no entrainment at all. (See fig. 6.9 pl. XIV.) In the unsteady

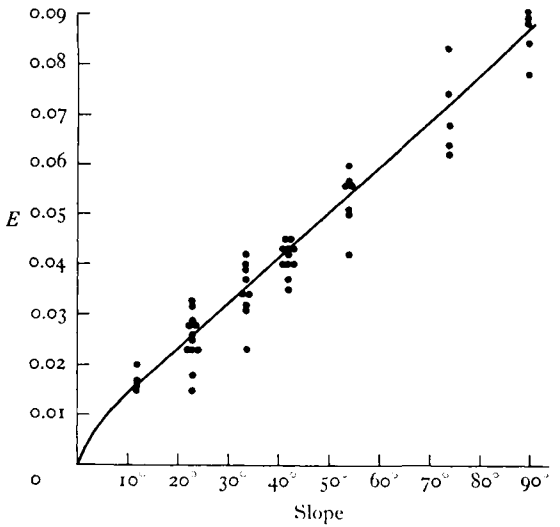

Fig. 6.10. Measurements of entrainment into an inclined plume as a function of slope. (From Ellison and Turner 1959.)

case, when the layer flow is preceded by a nose, the front of the flow itself acts as a control which keeps Ri_0 close to unity. (See §3.2.4.)

The second kind of experiment is the one illustrated in fig. 6.7, the inclined plume of salt water on a slope, to which the theory applies more directly. Here a steady plume can be set up, and the inflow of fresh water necessary to make up for the entrainment is measured as a function of slope. The results obtained in this way by Ellison and Turner are shown in fig. 6.10; the general dependence of E on slope is clear, but there is considerable experimental scatter attributed to the fact that the Reynolds number was not always large, and a layer of heavy fluid near the wall could sometimes remain non-turbulent.

The mean experimental results for E as a function of Ri_0 are plotted on logarithmic scales in fig. 6.8. At the smaller values of Ri_0 the surface jet results and those for inclined plumes obtained by Ellison and Turner are seen to be in good agreement. At the higher values of Ri_0, the curve is that due to Lofquist (1960), who studied an undercurrent on a much larger scale. Since this was maintained in a turbulent state by bottom friction, some measure of the roughness must also be a relevant parameter here. The two sets of results

do seem to be consistent with one another (though there is a gap not covered by any experiments), and with the assumption that a stability parameter like Ri_0 is the major factor determining the entrainment rate in both cases. We must, however, sound here the warning that at high values of Ri_0 molecular diffusion may play a significant role in the mixing process (see §9.1.3).

The laboratory results may be used confidently to make predictions of the velocity of flow of a larger scale turbulent gravity current on a steep slope. All that is required is an estimate of the rate of output of light or heavy fluid A; small changes in Ri_n due to Reynolds number effects or changes in friction coefficient are unimportant since U is proportional to $(A/Ri_n)^{\frac{1}{3}}$. (The constant of proportionality can be obtained as a function of slope from the laboratory experiments.) At low slopes, E becomes very small so that even at large Reynolds numbers there should be negligible friction at the interface. The weight of the layer must then be balanced solely by friction at the solid wall and

$$S_2 \frac{A}{U^3} \sin\theta = C_D. \tag{6.2.11}$$

On intermediate slopes, both entrainment and bottom friction may be important in determining the friction and flowrate.

The results of the previous section can easily be extended to calculate the opposing (non-turbulent) flow U_a which would be required to reverse a gravity current, for example, the magnitude of the upper wind which could destroy a katabatic wind at the surface, or the ventilating flow needed in a mine to prevent a dangerous layer of methane flowing uphill along the roof of a sloping roadway (see §5.3.3). If U now denotes the difference between the layer velocity and the external flow (with Ri_0 again defined using U), the buoyancy flux becomes $A = g'h(U+U_a)$, and the 'normal' state is described by the following generalization of (6.2.8):

$$\left(1 + \tfrac{1}{2} S_1 Ri_0 \frac{U}{U+U_a}\right) E = S_2 Ri_0 \tan\theta - C_D \frac{(U+U_a)^2}{U^2} \operatorname{sgn}(U+U_a). \tag{6.2.12}$$

Note that the last term (the drag) depends on the sign of $(U+U_a)$, the velocity of the layer, which may be in either direction, with or against U_a.

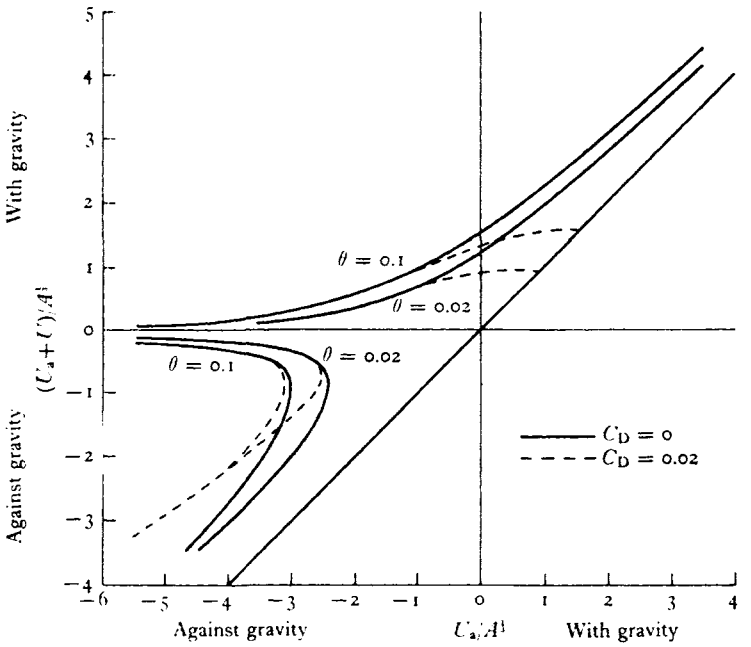

Fig. 6.11. Calculations of the velocity $(U+U_a)$ of an inclined plume entraining a moving ambient stream of velocity U_a. The empirical relation from fig. 6.8 has been used, and curves are shown for two slopes and two friction coefficients. (From Ellison and Turner 1959.)

For given values of θ and C_D and experimental values of $E(Ri_0)$, (6.2.12) may be solved numerically to give $(U+U_a)/A^{\frac{1}{3}}$ as a function of $U_a/A^{\frac{1}{3}}$, i.e. the non-dimensional layer velocity as a function of that in the ambient fluid, as shown in fig. 6.11. When U_a opposes the natural flow and is greater than about $3A^{\frac{1}{3}}$ (twice the downhill layer velocity in the absence of an opposing flow), the direction of layer flow can be reversed. The numerical constant varies only slowly with slope and friction coefficient, and this value has been verified by direct laboratory experiment. The Richardson number and hence the entrainment function and rate of spread do vary more markedly as the slope is changed. Small values of Ri_0 are relevant when the ambient flow is acting against gravity, whatever the magnitude of the slope, and the greatly increased mixing and stress in this state accounts for the sudden reversal of direction which is often observed. (Compare with §3.2.5.)

6.2.4. *Detailed profile measurements*

Though the experimental results of Ellison and Turner (1959) reported above were designed originally to obtain an 'overall' understanding of inclined plumes or bottom currents, they are sufficiently detailed to allow in addition an interpretation in terms of the local gradients. At moderately steep slopes the stress depends mostly on the entrainment at the outer edge of the layer and little on bottom friction (6.2.6). The turbulence effecting the entrainment is therefore produced in the same region as it is used to do work against buoyancy forces, and in this respect the flow is like the wakes discussed in § 5.3. Because of the component of gravity which tends to accelerate the flow if the stress becomes too small, one might expect in addition that this outer edge could be *maintained* in a marginally stable state. The theoretical argument of § 5.1.4 can be recast in terms of the local velocity and buoyancy differences across the edge of the plume to give

$$\frac{\mathrm{d}u}{\mathrm{d}z} = k_1 \frac{g'}{\Delta U}, \quad \frac{g}{\rho}\frac{\mathrm{d}\rho}{\mathrm{d}z} = k_2 \left(\frac{g'}{\Delta U}\right)^2. \tag{6.2.13}$$

Again it predicts linear profiles, essentially because no external lengthscale is relevant here.

Examination of the detailed measurements (such as those in fig. 6.12) shows that the outer edges of both the mean velocity and salinity profiles are indeed very closely linear. The whole of this outer region can be characterized by a single gradient Richardson number (corrected for the slope). For fifteen experiments in which reliable profiles were measured (with $\theta = 14°$ and $23°$) the range of values of $Ri \cos\theta$ was 0.044–0.077, with a mean value of 0.058. To the accuracy of the experiments they therefore support the existence of a critical gradient Richardson number, less than 0.1, at which turbulence is strongly damped.

6.3. Thermals in a uniform environment

6.3.1. *Dimensional arguments and laboratory experiments*

Similarity solutions can also be written down to describe the motion of axisymmetric thermals, or suddenly released regions of buoyant

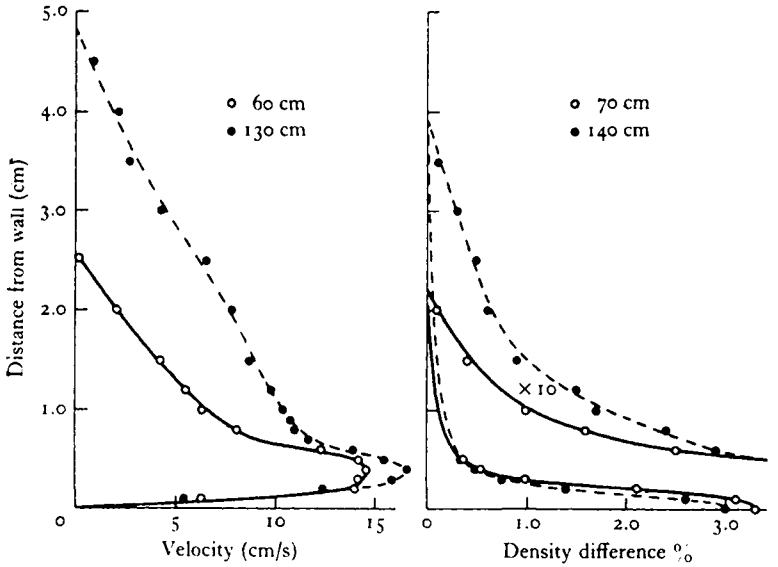

Fig. 6.12. Typical profiles of (*a*) velocity and (*b*) density in an inclined plume on a slope of 14°. (From Ellison and Turner 1959.)

fluid, as they rise and mix with their surroundings of constant density ρ_0. (It should be noted immediately that such solutions are less likely to be strictly applicable to real flows than is the case for plumes, since thermals typically grow to only a few times their original diameter and therefore do not have time to adjust to an equilibrium state.) Underlying these solutions is the assumption of similar distributions of velocity and buoyancy relative to the moving centre, and the sole parameter governing the motion is the total weight deficiency or buoyancy say $F_* = g(\rho_0 - \rho)V_0/\rho_0$, where ρ and V_0 are the initial density and volume of source fluid. The solutions for the typical horizontal dimension r_*, the mean vertical velocity w and g' in terms of powers of x and F_* (which is a constant in uniform surroundings) are

$$\left.\begin{aligned} r_* &= \alpha z, \\ w &= F_*^{\frac{1}{2}} z^{-1} f_1\left(\frac{\mathbf{r}}{r_*}\right), \\ g' &= F_* z^{-3} f_2\left(\frac{\mathbf{r}}{r_*}\right). \end{aligned}\right\} \qquad (6.3.1)$$

The profiles are functions of the vector position $\mathbf{r}$, which have so far only been obtained by experiment.

Scorer (1957) checked various consequences of this solution in laboratory experiments, using thermals of heavy salt solution falling through fresh water. He expressed his results in terms of the direct relation between the velocity $w_c = dz_c/dt$ of the cap of the thermal, the extreme horizontal radius b, and g' as

$$w_c = C(g'b)^{\frac{1}{2}}, \tag{6.3.2}$$

and also verified that

$$b \propto t^{\frac{1}{2}} \quad \text{and} \quad w_c \propto t^{-\frac{1}{2}} \tag{6.3.3}$$

which follow by writing (6.3.1) in terms of time instead of height. He found that the typical shape of thermals is a slightly oblate spheroid, with $m = V/b^3 = 3$. In any given experiment C (which has the form of a Froude number – compare (6.1.12)) and α $(= b/z_c)$ remain constant with time, but there can be large variations in angle of spread from one experiment to another; the mean values given were $C = 1.2$ and $\alpha = 0.25$. It can be shown (Turner 1964*b*) that there is in fact a relation between C and α, which is determined using only the shape of the thermal and the assumption of a potential flow around it, without requiring any information about the flow inside.

More detailed experiments have shown that the mean motion inside a thermal does remain approximately similar at all heights and is rather like that in a flattened Hill's spherical vortex, with an upflow at the centre (in a rising thermal) and descent near the edges (see fig. 6.13 pl. xv). The kinematic consequences of applying the exact spherical vortex model are illustrated in fig. 6.14. The surrounding flow is instantaneously the same as that in a perfect fluid round a solid sphere, but superimposed on this is a constant rate of inflow across the sharp boundary separating the turbulent interior from the surroundings. No 'skin friction' is possible here because any boundary layer is immediately incorporated into the thermal; the only drag arises because of the external fluid which must be accelerated from rest, either by being added to the thermal or displaced around it. The figure shows both the particle paths relative to the boundary and the shapes into which originally horizontal surfaces are distorted as the vortex overtakes them. Mixing may be enhanced at the front where the entrained fluid is

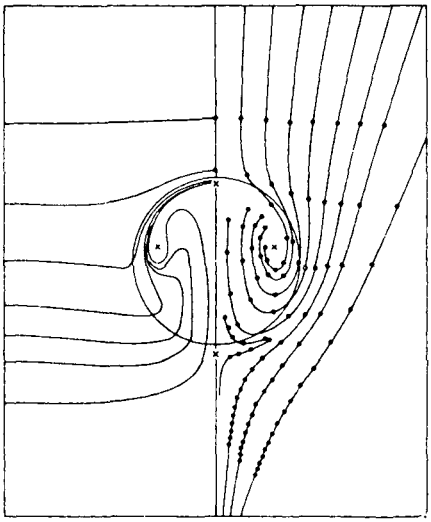

Fig. 6.14. The motion of particles into an expanding Hill's spherical vortex (right) and the distortion of initially horizontal planes of fluid (left) plotted in coordinates in which the spherical boundary is fixed in size. The tangent of the half angle of spread is $\alpha = \frac{1}{4}$. (From Turner 1964*a*.)

swept sideways in a thin layer (because the density contrast is statically unstable there), but there is also a broader region of inflow at the rear. Another result, which follows when the explicit spherical vortex velocity profiles are added to the similarity solutions, is worth a mention here. Only a fraction ($\frac{5}{14}$) of the work done by buoyancy appears as kinetic energy of mean motion, distributed between the 'solid' forward motion ($\frac{1}{6}$), the internal circulation ($\frac{3}{28}$) and the displaced external fluid ($\frac{1}{12}$); the balance ($\frac{9}{14}$) must go into turbulence and is eventually dissipated. (See Turner 1972.)

6.3.2. *Buoyant vortex rings*

A thermal released from rest can be regarded as a special case of a buoyant vortex ring (Turner 1957). For a thermal, the circulation is generated entirely by buoyancy, whereas in a vortex ring the initial buoyancy F_* and circulation K_0 can be specified separately at the source. When a volume of buoyant fluid is forcibly ejected upwards into uniform surroundings at rest, a vortex ring is formed in which both the vorticity and light fluid are contained within a sharp core.

This can either be laminar, and have a constant volume, getting thinner as the ring expands sideways, or turbulent, in which case the radius of its cross-section increases and remains nearly proportional to the radius R of the ring. (See fig. 6.15 pl. xv.) The cores are, however, carrying along with them a spheroidal region of non-buoyant fluid, rather like a thermal in shape.

One can take a circuit passing along the axis of the ring which contains only particles of fluid of constant density, so the circulation $K_0 \propto wR$ will remain constant in time. (This is true also for thermals, from the solutions (6.3.1). In that case it can be explained in terms of the balance between the generation of vorticity by buoyancy along the axis, and its destruction by mixing of vorticity of opposite signs across the centre-line.) The total impulse P of a vortex and its surroundings is

$$P = \pi\rho K_0 R^2. \tag{6.3.4}$$

If we suppose that this is being increased by the action of the constant buoyancy force F_*, then the momentum equation may be written as

$$\frac{\mathrm{d}P}{\mathrm{d}t} = \pi\rho K_0 \frac{\mathrm{d}R^2}{\mathrm{d}t} = \rho F_* \tag{6.3.5}$$

which gives

$$R^2 - R_0^2 = \frac{F_* t}{\pi K_0}. \tag{6.3.6}$$

With the additional assumption that the velocity distribution remains similar at all heights, so that $w = cK_0/R$, it follows that

$$R = \alpha z = \frac{F_*}{2\pi c K_0^2} z. \tag{6.3.7}$$

Thus the angle of spread of a vortex (and the special case of a thermal) is proportional to F_*/K_0^2. The release of a thermal from rest generates, during the process of acceleration, a relatively small value of K_0 and therefore a large angle of spread. Small differences in the manner of release can produce a different K_0, and a range of different angles, but once the similarity state is attained F_*/K_0^2 stays constant. Increasing K_0 for a given F_* (by giving extra momentum at the source) leads to a smaller angle of spread and hence less mixing with the environment. This is a very different behaviour from that of plumes, where extra momentum was seen to make the flow more jet-like and the spread greater (see fig. 6.5).

It is sometimes useful to formulate the dynamics of thermals and buoyant vortex rings in terms of the entrainment assumption (though as we have seen above, the total rate of addition of external fluid follows from a consideration of the overall dynamics, without mentioning the detailed mixing). If the inflow velocity is assumed proportional to the mean upward velocity of the centre w_0 and to the surface area, then one obtains a set of equations analogous to (6.1.6), which for a spherical thermal are

$$\left.\begin{aligned} \mathrm{d}b^3/\mathrm{d}t &= 3\alpha b^2 w_0, \\ \mathrm{d}(b^3 w_0)/\mathrm{d}t &= \tfrac{2}{3} b^3 g', \\ \mathrm{d}(b^3 g')/\mathrm{d}t &= -b^3 w_0 N^2. \end{aligned}\right\} \tag{6.3.8}$$

In writing these forms the thermal has been treated as if it were a well-mixed sphere and the 'virtual mass coefficient' appropriate to a sphere has been used, but only the multiplying constants will be changed if the properties are defined by integrating over observed distributions.

The first of (6.3.8) shows immediately that $b = \alpha z$, i.e. the entrainment assumption plus the equation of continuity alone implies a linear spread (whatever the properties of the environment); moreover for a spherical thermal the entrainment constant and the angle of spread are identical. (Contrast this result with (6.1.8).) If V is the volume of the thermal, it also follows that

$$V^{-1}\frac{\mathrm{d}V}{\mathrm{d}z} = \frac{3\alpha}{b}. \tag{6.3.9}$$

As for plumes (6.1.7) the proportional rate of entrainment depends inversely on the radius, but the rate of dilution of a thermal is much larger than it is for plumes, since α is larger.

6.3.3. '*Starting plumes*'

As mentioned in the introduction to this chapter, and sketched in fig. 6.1, a phenomenon related to both plumes and thermals is observed when a steady source of buoyancy is suddenly turned on, producing what has been called a 'starting plume'. This flow pattern stays similar at all times, but with increasing size; well behind the front the motion is just that in a steady plume, and at the front it is

like a thermal. (See fig. 6.16 pl. xv.) At first sight it seems unlikely that these flows could stay together, since the velocity dependence on height in (6.1.6) and (6.3.1) is quite different; but the appropriate thermal solution is not that for constant total buoyancy, since allowance must be made for the buoyancy and momentum fed into the cap from the plume behind. Here it is appropriate to use Gaussian profiles in the plume since this form gives a good match to that at the bottom of a spherical vortex.

With these modified assumptions one can obtain a detailed understanding of the similarity solution near the cap in terms of the separate plume and thermal dynamics, using the vortex ring equation (6.3.5) (Turner 1962). Again, certain parameters have only been obtained by experiment. The cap spreads with a half angle of $\alpha_0 = 0.18$ (defined as the maximum radius divided by the corresponding height), much less than the mean value of $\alpha_0 = 0.30$ defined in the same way for ordinary thermals. To preserve similarity the cap velocity must follow the power law appropriate to a plume, and it has a mean value of 0.61 times the velocity at the centre of the established plume at the same height. Although it may look like an isolated thermal from above, a plume cap dilutes only about one third as rapidly for a given size, because about half the fluid entering it comes from the plume below. The density difference will follow the plume dilution law, rather than that in a thermal.

6.3.4. *Line thermals and bent-over plumes*

Two-dimensional thermals have also received some attention, and they have a practical significance, since a section of a plume bent over by a (non-turbulent) wind will behave rather like a line thermal (provided we are able to ignore the differential velocity in the downwind direction which caused the plume to bend over in the first place). Richards (1963) performed laboratory experiments with line thermals released from rest which supported a similarity assumption, including a linear spread with height of the turbulent buoyant region (at a much greater angle than axially symmetric thermals). The physically relevant parameter for a bent over plume is now the buoyancy per unit length F_1, which is related to the buoyancy flux $F_0 = \pi F$ from the source by $F_1 = F_0/U$ where U is the

wind velocity (supposed constant with height). Dimensional arguments show that the height of rise z in time t is therefore

$$z \propto F_1^{\frac{1}{3}} t^{\frac{2}{3}}. \tag{6.3.10}$$

This can be put in terms of F and the distance $x = Ut$ downwind, giving

$$z = 1.6 F^{\frac{1}{3}} U^{-1} x^{\frac{2}{3}}. \tag{6.3.11}$$

The numerical constant has been added using the summary of observations in the atmosphere given by Briggs (1969), which also support the functional form (6.3.11) in an intermediate range of the total rise of a bent-over plume.

Alternatively one can approach the problem using a theory of buoyant vortex pairs analogous to the vortex ring case, assuming that the circulation K_0 as well as the buoyancy per unit length F_1 remain constant in time (Turner 1960*a*). Because of the different dimensions of F_1 this is not now equivalent to the similarity assumption; another length must enter the problem. It follows using the momentum equation

$$\frac{\mathrm{d}P_1}{\mathrm{d}t} = 2\rho K_0 \frac{\mathrm{d}R}{\mathrm{d}t} = \rho F_1 \tag{6.3.12}$$

that R spreads linearly in time, and therefore with distance downwind. Adding the expression for the velocity of a pair vortex $w = K_0/4\pi R$ shows that the radius increases exponentially with height

$$\frac{R}{R_0} = \exp\left(\frac{2\pi F_1}{K_0^2} h\right), \tag{6.3.13}$$

where h is the height between states with radii R_0 and R.

The apparent conflict between these two ideas was resolved by Lilly (1964) who showed (using a numerical model) that the behaviour depends on the relative magnitudes of turbulent diffusion and the rate of increase of R. If buoyant fluid and vorticity mix across the centre of the thermal, K varies but a linear spread of R with z is obtained; if they stay separate in two distinct cores, K remains constant and the vortex pair theory is appropriate. Both laboratory plumes and occasionally smoke from chimneys are observed to split sideways as they bend over away from the outlet, and in these cases the second model should be used.

Experiments have also been carried out with line thermals travelling along a solid boundary, either in isolation or as 'noses' at the front of turbulent gravity currents. When the wall is vertical the latter is equivalent to a two-dimensional starting plume (Tsang 1970) for which a similarity solution can again be found. The cap moves at only 0.38 times the maximum velocity of the steady plume behind it, and (unlike the axisymmetric case) spreads at a much faster rate than the plume behind, with $\alpha = 0.33$. As the slope of the boundary is decreased towards zero, a turbulent front persists, still moving rather more slowly than the flow behind, but not now so closely connected with it (see §3.2.4). The nose is flattened and spreads out backwards along the top of the steady flow and can be mixed into it again. Little attention has been given to this problem of mixing near turbulent fronts, compared to the inviscid (hydraulic) theories of chapter 3 or the mixing of the steady gravity currents described in §6.2.

6.4. The non-uniform environment

6.4.1. *Motions in an unstable environment*

Similarity arguments (or the equivalent entrainment assumption) can also be used to derive some of the features of convection from small sources in non-neutral conditions. Batchelor (1954*a*) showed that power law solutions can again be obtained for an environment whose density gradient is of the form

$$\frac{g}{\rho_1}\left(\frac{\mathrm{d}\rho_0}{\mathrm{d}z}\right) = Cz^p. \tag{6.4.1}$$

The constant C must be positive for this kind of solution to hold, implying that the environment must be unstable; the solution for stable surroundings will be considered separately. If a plume is supposed to arise from a small source at $z = 0$, then the variations of plume properties with height, consistent with (6.4.1) and the entrainment equations (6.1.6), are

$$\left.\begin{aligned} \overline{w} &= C^{\frac{1}{2}}(4+p)^{-\frac{1}{2}}(4+\tfrac{3}{2}p)^{-\frac{1}{2}}z^{(1+\frac{1}{2}p)}, \\ g' &= C(4+\tfrac{3}{2}p)^{-1}z^{(1+p)}, \\ b &= 2\alpha(3+\tfrac{1}{2}p)^{-1}z. \end{aligned}\right\} \tag{6.4.2}$$

Various special cases can be recovered by choosing the value of p. Notice that for all $p > -\frac{5}{3}$, the buoyancy flux at $z = 0$ is zero, so plumes of this kind can arise spontaneously from small disturbance in the environment, and no extra parameter specifying the initial buoyancy flux is needed. When $p = -\frac{5}{3}$, the equations can only be satisfied with $C = 0$, in which case the whole analysis reduces to that for a uniform environment (and the buoyancy flux is a relevant parameter). With $p = -\frac{4}{3}$ one obtains the solutions for plumes in conditions of 'free convection' (see §5.1.3) which can be used (as in §7.3) to give a detailed interpretation of the flux from a heated plane.

The discussion of thermals in unstable power law gradients can be carried through in the same way, though it is less interesting here: because disturbances can grow spontaneously, a continuing plume is more likely to develop than an isolated thermal. Line plumes are, however, of some practical importance in the atmosphere under unstable conditions since observations suggest that plumes from local hot spots tend to get drawn out into lines downwind.

The power law solutions (6.4.2) for plumes and the corresponding ones for thermals can also be used in some situations where the environment is conditionally unstable, for example because of the release of latent heat in the atmosphere. The important feature is that the density *difference* is changing in a certain way, and this may be achieved by a process of internal generation of buoyancy, even when the environment is uniformly or stably stratified. (A necessary qualification in stable stratification is that the momentum carried away by internal gravity waves should be small; see §6.4.3.) Using the chemical release of gas bubbles in a liquid to simulate latent heat, Turner (1963*a*) produced laboratory thermals which can be described in this way. These were unstable in the sense that they accelerated, but they did not lead to the formation of a continuing plume.

The processes of generation of buoyancy due to condensation and dilution due to mixing with the environment are basic to the understanding of the dynamics of clouds. Much of the work on convection in conditionally unstable surroundings has been carried out with this application in mind, and many of the theoretical models used by meteorologists have been based on, or can be reformulated in

terms of, the entrainment assumption. The original application of the simple 'thermal' experiments was to small clouds, but the practical situations are so complex that simple exact solutions do not take us far, and the details of more complicated models have been worked out numerically. (See, for example, Ogura (1963) for a conditionally unstable thermal calculation.) It is outside the scope of this book to pursue this subject far, but some results of more general interest should be mentioned.

In the case of a simple plume, Morton (1956) added an equation of continuity for moisture to the other three equations (6.1.4) and showed how the solution for a point source of various strengths can be modified by the presence of condensing water. His ideas were applied by Squires and Turner (1962) to a steady plume model of a cumulonimbus cloud. They specified the mass flux over a finite area at cloudbase, with given environmental properties, and calculated the vertical velocity, the liquid water concentration and height of penetration. This model may be applicable to individual updraughts within the cloud, but it is unlikely to be valid (as originally suggested) if the whole cloud is treated as single plume. A recent evaluation by Warner (1970) has shown that this and related steady-state 'entrainment' models are inadequate when they are tested against measurements in clouds. It is impossible to predict both liquid water concentrations and heights of penetration simultaneously, and there is some doubt whether the dilution depends simply on size in the manner suggested by (6.1.7). In retrospect, it seems clear that clouds (which are typically nearly as broad as they are tall) will not achieve a fully developed state, and are poor candidates for the application of similarity theories which describe the steady flow many diameters above a small source. 'Starting plume' models (§6.3.3) allow to some extent for mixing at the top as well as the sides, but this is not enough; a fully time-dependent approach is needed which treats a cloud as a whole and takes the non-equilibrium lateral entrainment properly into account.

6.4.2. *Plumes in a stable environment*

It is clear that the ordinary kind of similarity solution, expressing plume properties in powers of the height above the source, cannot

be found in a stable environment, since the buoyant fluid must come to rest at some finite height. There is no such limitation on the equations (6.1.6) based on the entrainment assumption. A useful case to discuss in detail (following Morton, Taylor and Turner 1956) is again the point source, with initial buoyancy flux $\rho_1 F_0$, in a constant stable density gradient $G = N^2 = -(g/\rho_1)(\mathrm{d}\rho_0/\mathrm{d}z)$.

The buoyancy flux will now of course be decreasing with height, but the equations can be put into a non-dimensional form using the two governing parameters, F_0 at the source and G (or N). Denoting non-dimensional functions corresponding to height z, radius b, vertical velocity w and buoyancy parameter g' by a subscript 1, the following transformations

$$\left.\begin{aligned} z &= 0.410\alpha_G^{-\frac{1}{2}} F_0^{\frac{1}{4}} N^{-\frac{3}{4}} z_1, \\ b &= 0.819\alpha_G^{\frac{1}{2}} F_0^{\frac{1}{4}} N^{-\frac{3}{4}} b_1, \\ w &= 1.158\alpha_G^{-\frac{1}{2}} F_0^{\frac{1}{4}} N^{\frac{1}{4}} w_1, \\ g' &= 0.819\alpha_G^{-\frac{1}{2}} F_0^{\frac{1}{4}} N^{\frac{3}{4}} \Delta_1, \end{aligned}\right\} \tag{6.4.3}$$

reduce (6.1.6) to the convenient non-dimensional form

$$\frac{\mathrm{d}m_1}{\mathrm{d}z_1} = v_1, \quad \frac{\mathrm{d}v_1^4}{\mathrm{d}z_1} = f_1 m_1, \quad \frac{\mathrm{d}f_1}{\mathrm{d}z_1} = -m_1. \tag{6.4.4}$$

The numerical factors in (6.4.3) are those appropriate to a value of α_G defined for Gaussian profiles, and the new functions in (6.4.4) are related to the physically relevant mass, momentum and buoyancy fluxes by

$$m_1 = b_1^2 w_1, \quad v_1 = b_1 w_1, \quad f_1 = m_1 \Delta_1. \tag{6.4.5}$$

The numerical solutions of the equations (6.4.4), with the boundary conditions $m_1 = 0, v_1 = 0, f_1 = 1$ and $z_1 = 0$ (corresponding to a virtual point source of buoyancy alone) are shown in fig. 6.17(*a*). Up to $z_1 = 2.0$ the plume spreads nearly linearly, and the solutions are little different from those in a neutral environment, but above this height it spreads more rapidly sideways. In this region the entrainment formulation becomes more questionable, and the plume must also overshoot and fall back; a fuller discussion of this behaviour is given below. Ignoring these difficulties for the moment, values for two heights are obtained from the solutions: $z_1 = 2.13$

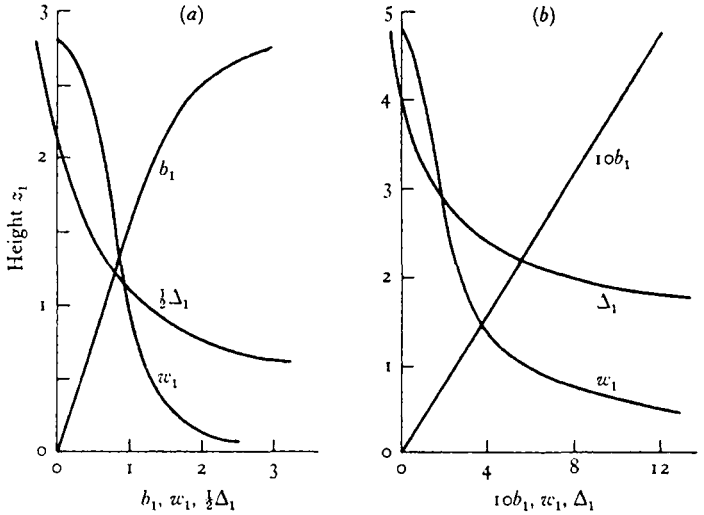

Fig. 6.17. The non-dimensional solutions for the width b_1, the vertical velocity w_1 and the buoyancy parameter Δ_1, as a function of height z_1 for (*a*) a plume and (*b*) a thermal in a linearly stratified environment. (After Morton, Taylor and Turner 1956.)

where the density difference first vanishes, and $z_1 = 2.8$ where the vertical velocity vanishes. (These are also marked on fig. 6.2.)

The top of the layer of fluid flowing out sideways will lie somewhere between these levels; substituting in (6.4.3), with the experimentally determined value of α_G (see §6.1), gives a numerical estimate for the final height. Uncertainties about the multiplying constant can be removed by direct experiment. As shown in fig. 6.18, Briggs (1969) has found that the formula

$$z_{\max} = 5.0F^{\frac{1}{4}}G^{-\frac{3}{8}} \tag{6.4.6}$$

gives good agreement with observations over a wide range of scales, from the laboratory to a plume above a large oil fire. Note that $F = F_0/\pi$ has been used here (instead of F_0 as in (6.4.3)) and of course potential density gradients are implied for all the measurements in the atmosphere.

Detailed observations near the top of a plume in a stable environment have been made by Abraham and Eysink (1969), and they can be interpreted using a model related to our fig. 6.6. As in a uniform

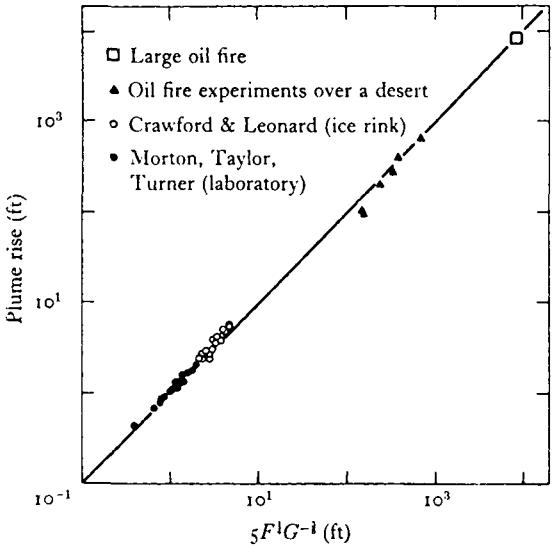

Fig. 6.18. Measurements of plume rise in calm stratified surroundings compared with the relation (6.4.6). (From Briggs (1969), where the various sources of data are discussed more fully.)

fluid, excess momentum causes the plume to continue rising in the centre, past the level of zero buoyancy. It forms a dome on top, then falls back in an annular region surrounding the upflow and finally spreads out horizontally (see fig. 6.2 pl. XIV). At all levels above the height where the plume density first equals that of the environment, the density on the centreline remains substantially constant, showing that the spreading layer protects the core of the plume from further mixing with the environment.

In this context of a stable environment, we should also refer to a different formulation of the problem by Priestley and Ball (1955), which leads to essentially the same predictions for the final height though it is based on rather different assumptions. Instead of entrainment, they assumed similarity of the profiles of shear stress and a quadratic dependence of stress on mean velocity. An acceleration-dependent term is thereby added to the mass-continuity equation (the first of (6.1.6)), but otherwise the equations are the same. (See Priestley 1959, p. 79.) Both theories break down near the plume top, though the limiting behaviour predicted by them is different. In the case of the Priestley and Ball model, the shape of the

plume depends on the form of the profile adopted. For example, the spread is linear if the profiles are Gaussian, whatever the density gradient in the environment, whereas 'top hat' profiles give an increased sideways spreading in stable surroundings. When the entrainment assumption is made, however, this latter behaviour is predicted (perhaps more realistically) as an integral property of the flow, regardless of the particular profile chosen.

6.4.3. *Forced plumes and vortex rings in a stable environment*

The theory of forced plumes described in §6.1.4 can be extended to include the case of a linear density stratification. Since there are now three governing parameters, the momentum and buoyancy fluxes M_0 and F_0 at the source, plus the stratification parameter G, not all of these can be removed by making the equations non-dimensional. Morton (1959*a*) took $\sigma = GM_0^2/(F_0^2 + GM_0^2)$ as the additional non-dimensional parameter, and solved a series of problems for virtual point sources of various kinds over the range $0 < \sigma < 1$.

His solutions are shown in fig. 6.19. The most striking result is that for upward directed buoyancy and momentum fluxes, the addition of some extra momentum to a buoyant plume can actually slightly decrease the total height to which it will rise in stable conditions, because of the greater mixing produced near the source when the flow is more like a jet (see (6.1.8)). Only at much larger values of M_0 (as $\sigma \to 1$) is this effect reversed so that the plume top will rise again; the result suggests that the continuous discharge of chimney gases at high velocities is not a practical way to increase plume heights (or to reduce pollution).

A similar analysis to that leading to fig. 6.17(*a*) has been carried out, based on the entrainment assumption, for thermals released into a linearly stratified environment. (For details see Morton, Taylor and Turner (1956).) The non-dimensional solutions found in this way are shown in fig. 6.17(*b*). The final height is of the form

$$z_{\max} \propto \alpha^{-\frac{3}{4}} F_*^{\frac{1}{4}} G^{-\frac{1}{4}} = 2.66 F_*^{\frac{1}{4}} G^{-\frac{1}{4}}. \qquad (6.4.7)$$

The multiplying constant, taken from laboratory experiments, is in reasonable agreement with the theoretical predictions using the

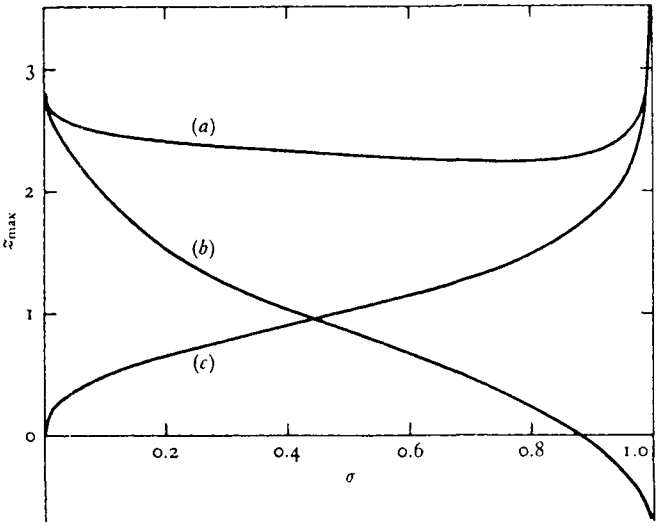

Fig. 6.19. Forced plumes in a stably stratified environment showing the final heights achieved as a function of the parameter σ for sources with (*a*) positive buoyancy and upward momentum, (*b*) positive buoyancy and downward momentum and (*c*) negative buoyancy and upward momentum. (From Morton 1959*a*).

value of α previously obtained for thermals in a neutral environment.

For thermals, the equivalent of the forced plume is a buoyant vortex ring with arbitrary initial buoyancy F_* and circulation K_0. With the similarity assumption, the angle of spread remains constant and proportional to F_*/K_0^2 (6.3.7) in a stratified environment. Substituting this in (6.4.7) shows that

$$z_{\max} \propto F_*^{-\frac{1}{2}} K_0^{\frac{3}{2}} G^{-\frac{1}{4}}. \tag{6.4.8}$$

The curious feature of a decrease in final height with increasing buoyancy, for fixed K_0, has been confirmed by laboratory experiment.

The most important property of (6.4.8) is the sensitive dependence on the initial circulation. Increasing K_0 (and hence reducing the angle of spread, and the rate of mixing) can lead to very large increases in the final height to which buoyant material could rise in stable surroundings. Such increases have indeed been observed for large explosion clouds, and the result is the basis for suggestions

(Turner 1960*b*, Fohl 1967) that waste gases should be ejected from chimneys intermittently rather than continuously in very stable conditions. The contrast between plumes, for which extra momentum has an adverse effect (fig. 6.19) and vortex rings, where there is in principle a great advantage to be gained, is very marked.

The same remarks do not apply to plumes bent over by a (non-turbulent) cross wind, where the evidence suggests that an extra rise can be produced by increasing the efflux velocity. This too can be interpreted in terms of the 'line thermal' model of a bent-over plume. Following the argument used in §6.3.4 for neutral surroundings, the total rise of a bent-over plume driven by buoyancy alone must depend on $F_1 = F_0/U$ and G. On dimensional grounds it must be of the form

$$z_{\max} \propto (F_0/UG)^{\frac{1}{3}}. \tag{6.4.9}$$

Extra vertical momentum injected during the first part of the bent-over phase can decrease the angle of spread and increase the total rise as before.

The simple entrainment assumption gives a poor representation of the behaviour of thermals near the final height, but it can be replaced by separate physical assumptions about the variations of F_* and K_0 with height (Turner 1960*a*). These predict an increased spreading in stably stratified surroundings if the circulation falls to zero before the momentum, or a collapse if the momentum vanishes first. The latter behaviour seems to correspond to the phenomenon of 'erosion' observed when laboratory thermals (or cloud towers) come to rest in a stable gradient. Models which relate entrainment to the mean velocity certainly cannot take account of the effect observed by Grigg and Stewart (1963), and discussed in §5.2.2. They showed that a thermal can be brought to rest before the small scale motions are very much affected, and the latter will continue to produce some mixing even in the absence of a mean upward velocity. Another process which is left out of account in all these models is the wave drag, which becomes especially important when the buoyancy of the thermal reverses and it is oscillating about its equilibrium height (Warren 1960, Larsen 1969*b*).

6.4.4. *Environmental turbulence*

So far in this chapter the environment has been supposed to be at rest and completely unaffected by the passage of the buoyant elements through it. Surrounding fluid has been entrained into the plume or thermal by the self-generated turbulence, but no transfer has been contemplated in the other direction. This assumption will now be relaxed to allow for the removal of buoyant fluid by turbulence in the surroundings, though we still concentrate on the behaviour of the buoyant elements themselves, leaving the discussion of the complementary changes in the environment to §7.3.

Priestley (1953) introduced the concept of the *open parcel*, of fixed size, over whose (spherical) surface interchange of fluid is taking place at the same rate in each direction. Turbulence in the environment is thus assumed to dominate the whole of the mixing process, and if the region of interest is so large that its properties remain unchanged, the momentum and buoyancy equations can be written, following Priestley (1959, p. 74), in the form

$$\left.\begin{aligned} \frac{\mathrm{d}w}{\mathrm{d}t} &= g' - k_1 w, \\ \frac{\mathrm{d}g'}{\mathrm{d}t} &= -Gw - k_2 g'. \end{aligned}\right\} \tag{6.4.10}$$

The last term in each of these is a simple (but arbitrary) representation of the effect of the turbulent interchange, which is assumed to reduce w and g' at a rate proportional to their magnitude; k_1 and k_2 are defined as 'mixing rates' for momentum and buoyancy. These parameters have dimensions t^{-1} in this formulation and, Priestley argued, they can be regarded as inverse measures of the size of the parcel, since with a given level of turbulence it will take longer for the properties of the larger elements to change. The solutions of (6.4.10) can take three forms according to the relative magnitudes of the coefficients, which can be assumed constant for a given parcel. Small enough elements (large k_1 and k_2), starting with finite velocity or excess buoyancy, travel a finite distance whatever the sign of the density gradient G, and approach their final height asymptotically. When the parcel exceeds a critical size, two different modes of motion become possible. In stable conditions there

is an oscillltion about the final equilibrium height, in damped harmonic motion with period

$$T = 2\pi|G - \tfrac{1}{4}(k_1 - k_2)^2|^{-\frac{1}{2}}. \tag{6.4.11}$$

When $k_1 = k_2$ this is just $2\pi/N$, but when the mixing rates for momentum and buoyancy are different, the period is increased. In an unstable gradient large parcels accelerate, and solutions with exponentially increasing velocities are relevant.

The model just described takes no account of the entrainment due to self-generated turbulence which was the basis of the earlier sections. Both environmental turbulence and that due to the motion can be combined in an 'entrainment' type of model if it is assumed that the outflow velocity is constant, proportional to a characteristic velocity u_0 in the environment, while the inflow is again proportional to the mean vertical velocity. The radius b is retained as a variable, and an extra term describing the outflow is added to each of (6.3.8). The continuity equation gives immediately

$$b - b_0 = \alpha z - u_0 t, \tag{6.4.12}$$

so with these assumptions the increase of radius due to entrainment is reduced by the existence of an outflow.

The modified entrainment equations can be made non-dimensional using the initial total buoyancy F_* and u_0 as scaling parameters. The effect of stratification (described by constant $G = N^2$ say) is contained in the non-dimensional parameter $\gamma = -\frac{4}{9}\alpha G F_* u_0^{-4}$, and solutions have been obtained for point sources and a range of values of γ (Turner 1963*b*). When $G = \gamma = 0$, the radius increases to a maximum, then decreases to zero at

$$z_{\max} = 0.83 F_*^{\frac{1}{4}} u_0^{-1}. \tag{6.4.13}$$

This maximum height is in reasonable agreement with the results of laboratory experiments, provided u_0 is taken to be comparable with the r.m.s. turbulent velocity. Solutions for other values of γ are shown in fig. 6.20. In stable and also slightly unstable conditions they are like the neutral case; no oscillatory motion occurs now (in contrast to the result (6.4.11) obtained for the 'open parcel' model). At a value of γ of about 145, the behaviour changes markedly,

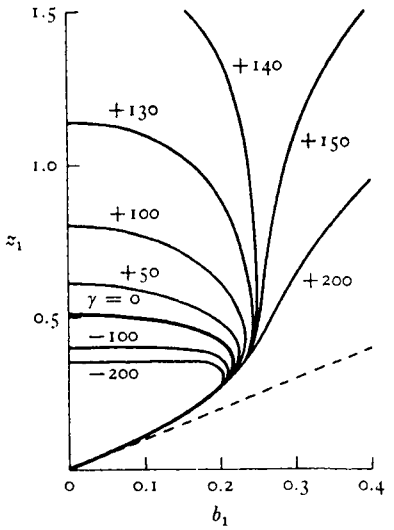

Fig. 6.20. The calculated behaviour of buoyant thermals in turbulent surroundings, for various values of the parameter $\gamma = -\frac{4}{9}\alpha G F_*/u_0^4$; positive values of γ correspond to unstable environments. (From Turner 1963*b*.)

and absolute instability becomes possible, just as with the 'open parcel'. This second formulation does, however, emphasize the sensitivity of the criterion for exponential growth to the level of turbulence in the environment, through the parameter $\gamma \propto u_0^{-4}$.

Another kind of buoyant element which has received some attention in a turbulent environment is the bent-over plume. Priestley (1956) considered this in two stages, the first when entrainment dominates (leading to (6.3.11)), with an abrupt transition to a state where the turbulence is everywhere the same as that in the environment, so that a two-dimensional form of 'open parcel' argument can be used. Slawson and Csanady (1967) suggested that it is useful to subdivide this latter range further. In the intermediate phase, turbulence in the inertial subrange is supposed to dominate the mixing, and the spreading rate depends on the plume radius b and on ϵ, the rate of energy dissipation (see §5.2.2 and Batchelor 1952). These assumptions imply an effective inflow velocity proportional to the velocity scale of eddies of radius b, and lead to the prediction that the plume will level off at an asymptotic height. In the final phase the eddy diffusivity is essentially constant, and the influx

velocity decreases as b increases. The asymptotic path of the plume is a straight line of fixed slope, a prediction which seems to agree with observations in the atmosphere in neutral conditions. These authors have also extended the model to stable and unstable stratification, and have shown that the intermediate phase can sometimes be important; this suggests that it may always be necessary to specify the scale of the motions considered, and not just a characteristic turbulent velocity of the environment.